<u>FULL PAPER</u>

Evaluation of fabricated IR absorbing films of polymer nanocapsules

Soraj A. Rahem* ⬡ |**Mohsin E. Aldokheily** |**Athraa H. Mekky**

Department of Chemistry, College of Science, University of Thi-Qar, Thi-Qar, Iraq

The objective of this study was to synthesize polymeric nanocapsules by microemulsions method that doping by different amines compounds to improve the properties of the polymer which consists of (dispersed) phase from ethyl acetate it inside, and the polymers is dissolved in it. In external (continuous) phase from water, these mix the two phases by surfactant etyltri methyl ammonium bromide (CTABr). In this study, the structures of polymer nanocapsules were identified by using X-Ray diffractogram (XRD) to calculate crystallite sizes (D) of the samples that were calculated using the Scherrer formula ranging up to the nano-size 17-50 nm. Likewise, studying the surface forms, morphology, and diameters of polymer nanoparticles by Scanning Electron Microscope (SEM) technology as well as the morphology of nanocapsule with high-resolution images of the sample, these images gave spherical and irregular shapes with the particles size and different diameter of 20-200 nm. Besides, using Infrared Spectroscopy (FT-IR) to characterize the functional groups of polyacrylicnanocapsule doped, proved the existence of new functional group C=O amide back to the reaction between polymer and amines. Proved the films of polymer pure and doped polymer nanocapsule have absorption photothermal properties by capability to absorb IR rays and calculate the temperatures by used thermometer device T-type to measure the amount of IR rays. The disparity in temperature back to pulling and propellant groups which direct the samples to absorb more or less IR rays. The nano samples are arranged according to their absorption of sunlight and IR lamp. They are arranged from the highest absorption to the lowest to sample of nanocapsul in IR sunlight and IR lamp: $SA_1 < SA_2 < SA_3 < SA_4 < SA$.

*Corresponding Author:
Soraj A. Rahem
Email: Qarsorajalirahem91@gmail.com
Tel.:+9647830920326

Introduction

The absorption of sunlight throw building materials and passage of IR through transparent surfaces such as windows is responsible for other in similar spaces [1]. The controlling excess of solar energy without compromising the visible transparency of the window is the important observance for health of human: maintaining inside/outside contact and natural lighting are essential to maintain productivity and well-being [2, 3]. The study concentrate on organic materials to absorb IR radiations on regulating windows which were made based on which can adjust the dependence on environmental conditions [4]. In IR window control systems. There are some advantages to employ organic rather than inorganic materials for instance, since they are non-

metallic, interfere with electromagnetic waves or they do not corrode [5–7].

Microemulsions are initially the great success stories of modern processing in chemistry. It is metastable colloidal scuttle consisting of two immiscible liquids [8] that are classified as oil-in water (O/W) or water-in-oil (W/O) depending on which phase constitutes the disperse phase. It can be prepared by different methods such as low energy emulsification, high-pressure, and others.

In this study, preparing nanocapsules of polyacrylic polymers, the nanocapsules differentshapes, different sizes of core and shell thickness with various surface morphologies are depended on emulsions method [9]. In addition, it can be spherical, centric, star-like, tubular, or eccentric in shape, depending on the shape and size, their properties regulation from material to another [10].

The development of nanomaterials and polymers capable of effectively to absorb the near-infrared (NIR) radiation with a broad working waveband has increasingly attracted the interest from the opinion of energy economization for applications in solar collectors, photothermal therapy, smart windows, and optical filters [12]. Solar energy is the most promising possible energy source between the existing sources of renewable energy and by using solar collectors; it can be converted into thermal energy [13]. In addition, we intended to modify the properties of polymers polyacrylic by doping with several various amines which have the great ability to absorb IR rays.

Experimental

Chemicals and instruments

The primary substances and solvents, in this study, were purchased from BDH and Sigma Aldrich companies, and they were used without further purification. Melting points were measured using a melting point apparatus and the uncorrected points were recognized.

The **FT-IR** spectra were recorded with KBr disk on "Perkin Elme, tensor 27 Bruker" in the range of (400-4000) cm^{-1} in the College of Science, University of Thi-Qar.

The **XRD** crystalline structure for any material can be recognized by studying the phase of (XRD) for that material, XRD Instrument. Generator Settings 40 mA, 40 kV, Anode Material (Cu), Panalytical Company-MODEL X' Pert Pro, Iran.

The **SEM** type of electron microscope captured images of a sample by scanning it with a high-energy beam of electron to produce signals that contain information about the sample's surface morphology, composition, etc. FESEM Instrument: ZEISS MODEL SIGMA VP, Iran.
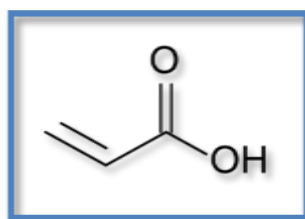
Preparation polymer nanocapsules

The preparation of emulsion nanocapsulesby organic phase (20 mL) of ethyl acetate and aqueous phase (80 mL) were mixed by mechanical stirrer for 24 hours. The mixture solvent was separated using separator funnel to obtain the saturated water containing ethyl acetate and the saturated solvent contained of water [10]. Polymer poly acrylic (0.5 g) and doping to 0.003 g of different amines compounds (Table 1) in ethyl acetate was saturated at 50 °C. The saturated water contained surfactant CATBr (1.00 g), the oil was added when the solution has cooled back to room temperature. The resulting organic solution was poured into the aqueous phase and emulsified with a rotor-stator device ultrasonic for 15 minutes. The oil-in-water emulsion (O/W) formed at temperature 10-20 °C. In the second step, the dispersed droplets were converted into nanocapsules in solvent diffusion. Furthermore, adding a large volume from water (4 times the volume of the emulsion) to the emulsion under gentle stirring with a magnetic bar after removing

ethyl acetate and part of water using rotary evaporator under reducing pressure. The obtained nanocapsules were purified by repetitive centrifugation, and then it was dried [14]. Scheme 1 displays the structures of Acrylic polymers.

TABLE 1 Symbol of pure samples polymer and polymer doping with different amines

Symbol	Compounds
SA	Polymer
SA$_1$	Polymer + 3-amino phenol
SA$_2$	Polymer + 4-Nitro aniline
SA$_3$	Polymer + 2-aminobenzoimidazole
SA$_4$	Polymer + 2-amino benzothiozole

SCHEME 1 Structures of acrylic polymers

Preparation films of polymers

The photothermal properties to films from polymer nanocapsule films to absorb IR of sunlight rays once and again by IR lamp was determined using T-type thermo-cables to measure the temperature in solid material which was applied on the films consisting of two layers, the first layer from polymer polyacrylic mixtures with his own resin, and the second layer consists of doped nano capsule polyacrylic polymer led to adding the prepared film to the only layer from polyacrylic polymer. Moreover, a wire is passed between the two layers to measure the absorbed temperature.

These films are exposed directly to sunlight rays (at air temperature 18 °C). Measurement the amount of absorbed IR was performed by using thermo-cables that record every 15-75 minutes. The films are again exposed to the IR lamp at distance more than a meter.

Results and discussion

Analysis of infrared spectroscopy FT-IR

The FT-IR spectra of sample **SA** polymerpolyacrylicin is displayed in Figure 1. The observed stretching vibration band was at 3002 cm^{-1} for OH$_{carboxylic\ acid}$, it was at 2963 cm^{-1} for =C-H$_{aliphatic}$ of methylene group, and at 2930, 2837 cm^{-1} for -C–H$_{aliphatic}$. It is notable that stretching vibration bands was at 1622 cm^{-1} for C=O$_{carboxylic\ acid}$. In addition, the stretching band was appeared at 1590-1508 cm^{-1} to C=C of methylene group and the bending out of plane at 1465-1416 cm^{-1}. Likewise, the stretching band was at 1344cm^{-1} for C-O.
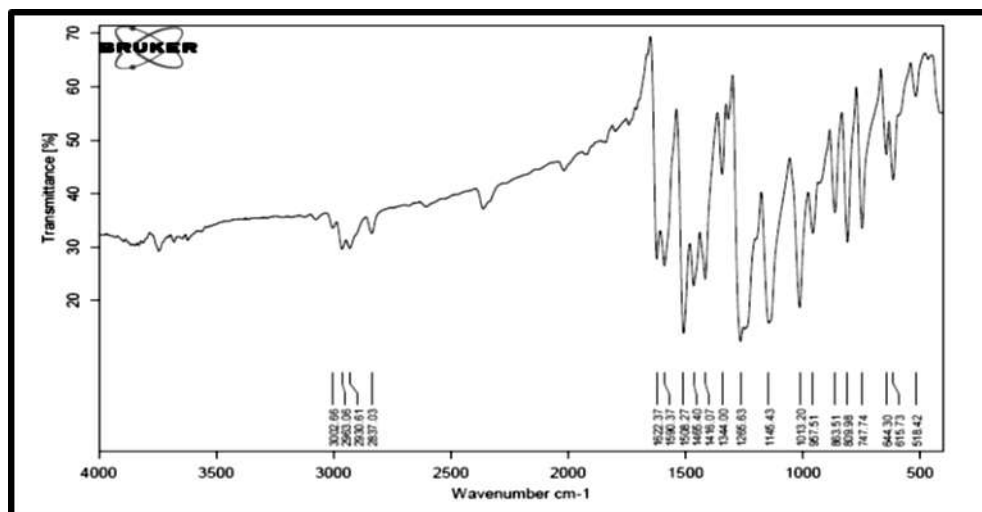
FIGURE 1 IR spectrum of sample SA polymer polyacrylic

In Figure 2, the FTIR spectra was indicated for sample **SA₁** of polymer nanocapsule doping with 3-Amino phenol. Also, two bends were weak at 3443 and 3361 cm⁻¹ for OH of amine, and two weak bends at 3304cm⁻¹ and 3205 cm⁻¹ for NH_2 back to amine. Additionally, the bend stretching vibration was appeared at 3012 cm⁻¹ back to C-H$_{aromatic}$, a stretching bend at 2919 cm⁻¹ for =C–H$_{aliphatic}$, and a bend stretching at 2850 cm⁻¹ to -C–H$_{aliphatic}$. Also, a bend stretching at 1730 cm⁻¹ of C=O$_{amide}$ returned to the reaction between polymer and amine. Likewise, a bend stretching vibration was observed at 1601 cm⁻¹and 1482 cm⁻¹ for C=C group of polymer. Also, a bend stretching was illustrated at 1271 cm⁻¹ and 1192 cm⁻¹ for C-N and C-O, respectively.
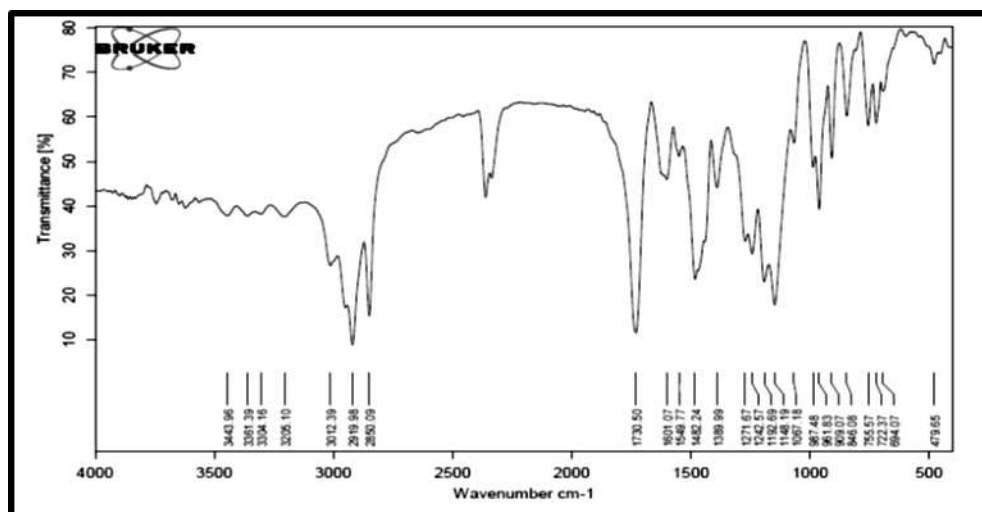

FIGURE 2 FTIR spectrum of sample **SA₁** polymer nanocapsule

The analysis of FT-IR spectrum was demonstrated in Figure 3 for sample **SA₂** of polymer nanocapsule doping with *P*-Nitro aniline. It is notable that two weak bends were observed at 3478 cm⁻¹ and 3361 cm⁻¹ for $NH_2$of amine, and at 3362cm⁻¹ and 3208cm⁻¹ for resonance. The bends stretching vibration were appeared at 3009 cm⁻¹ back to C-H$_{aromatic}$, and a stretching at 2950 cm⁻¹ for =C–H$_{aliphatic}$ for polymer, and bends stretching

at 2920 cm^{-1} and 2849cm^{-1} for C–H$_{aliphatic}$. Also, a bend stretching was indicated at 1730 cm^{-1} of C=O$_{amide}$ back to the reaction between polymer and amine, and a bend stretching at 1635 cm^{-1} and 1480 cm^{-1} for C=C group for polymer. In addition, two bends were stretching at 1596 cm^{-1}and 1390 cm^{-1} back to NO$_2$ and amine. Furthermore, a bend stretching was observed at 1273 cm^{-1} and 1307 cm^{-1} to C-N and C-O, respectively.
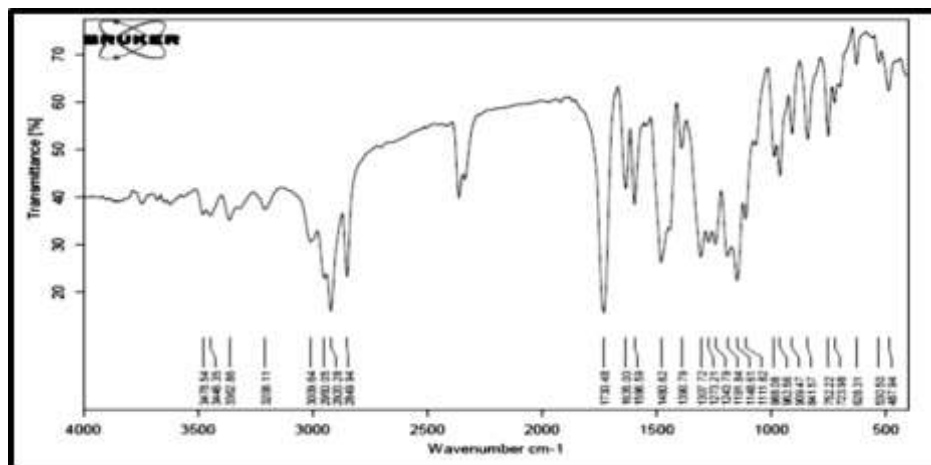

FIGURE 3 FTIR spectrum of sample SA2 polymer nanocapsule

As depicted in Figure 4, FTIR spectrum was performed for sample **SA$_3$** of polymer nanocapsule doping with 2-Amine benzoimidozol. It is notable that a bend stretching vibration was observed at 3124 cm^{-1} of NH of amine, a bend stretching vibration at 3014 cm^{-1} returned to C-H$_{aromatic}$, one at 2920 cm^{-1} for =C–H$_{aliphatic}$, and another one at 2849 cm^{-1} of C-H$_{aliphatic}$. Likewise, a bend stretching vibration was indicated at 1730 cm^{-1} of C=O$_{amide}$ back to the reaction between polymer and amine, another at 1546 cm^{-1} of C=N of amine, and a bend stretching at 1482 and 1452cm^{-1} for C=C group of polymer. In addition, a bending was observed at 1323 cm^{-1} and 1244 cm^{-1} to C-N and C-O, respectively.
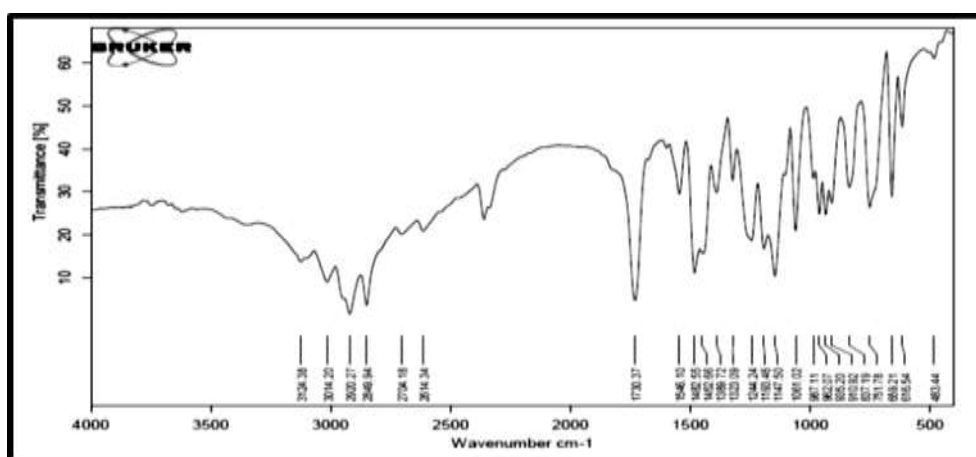

FIGURE 4 FTIR spectrum of sample **SA$_3$** polymer nanocapsule

As demonstrated in Figure 5, the analysis FTIR spectrum was carried out for sample **SA$_4$** of the prepared polymer nanocapsule doping with 2-Amine benzoimidothiozol. A bending was appeared at 3132 cm^{-1} of NH. It is noted that a bend stretching vibration was

indictaed at 3016 cm^{-1} back to C-H$_{aromatic}$, a bend stretching peak at 2946 cm^{-1} for =C–H$_{aliphatic}$, and bend stretching at 2918cm^{-1} and 2849cm^{-1} to -C–H$_{aliphatic}$. Also, a bend stretching was observed at 1732 cm^{-1} of C=O$_{amide}$ back to reaction between polymer and amine, one at 1646 cm^{-1} for C=N of amine, another at 1627cm^{-1} and 1487 cm^{-1} for C=C group for polymer, and a bend at 1541 cm^{-1} for C=S of amine. In addition, a bend was appeared at 1395 cm^{-1} and 1147 cm^{-1} for S-C as well as 1273cm^{-1} and 1244 cm^{-1} for C-N and C-O, respectively [16].
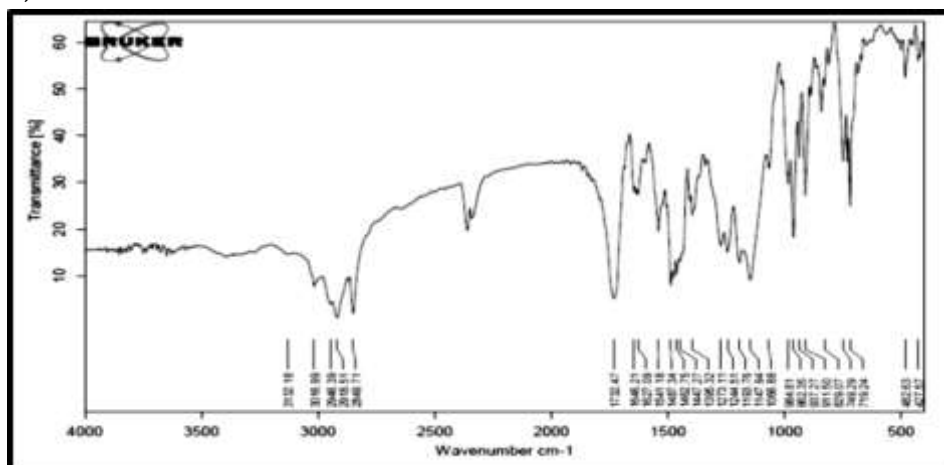

FIGURE 5 FTIR spectrum of sample **SA₄** polymer nanocapsules

X-Ray diffractogram techniques (XRD)

The X-ray diffractogram (XRD) analysis was performed to study structure and crystallite size for the polymer doping by Schiff bass synthesis, in which crystallite sizes are determined by Scherrerformula [17]:

$$D = \frac{K\lambda}{\beta\ COS\Theta}$$

Where K = 0.89 is shape factor, (λ) is wavelength of irradiation (Cu Kα = 0.154056 nm),(β)is (FWHM) and Θ is XRD diffractogram angle.

Figure 6 displays the XRD diffractogram of pure sample **SA** polymer as well as broad signals. The first highest peak was at 2Θ=13.2 with the intensity of 100% and crystal size=3.956 nm. The second highest peak was at 2Θ=30.9 with the intensity of 23.48% and crystal size=1.165. The third highest peak was at 2Θ=42.7 with the intensity of 11.90% and crystal size=2.110 nm [18].
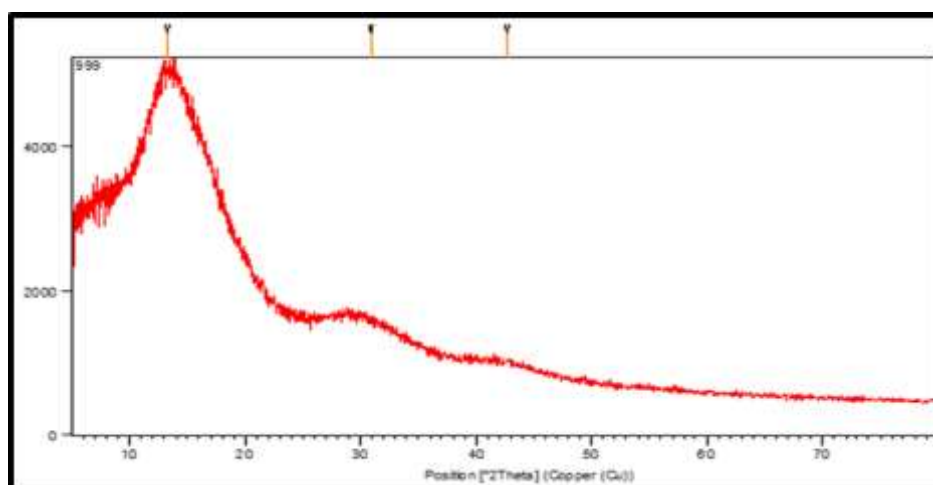

FIGURE 6 XRD diffractogram Spectrum of sample **SA** polymer polyacrylic

Figure 7 shows the XRD diffractogram of sample **SA₁** polymer nanocapsule as well as the given signals. The first highest was at 2θ=6.883 with the intensity of 100% and crystal size=57.898nm. The second highest peak was at 2θ=20.55 with the intensity of 54.72% and crystal size=43.685. The third highest peak was at 2θ=21.498 with the intensity of 48.47% and crystal size=58.842. The XRD patterns revealed the increasing number and density of peaks back to the element formation of polymer and amine [18].
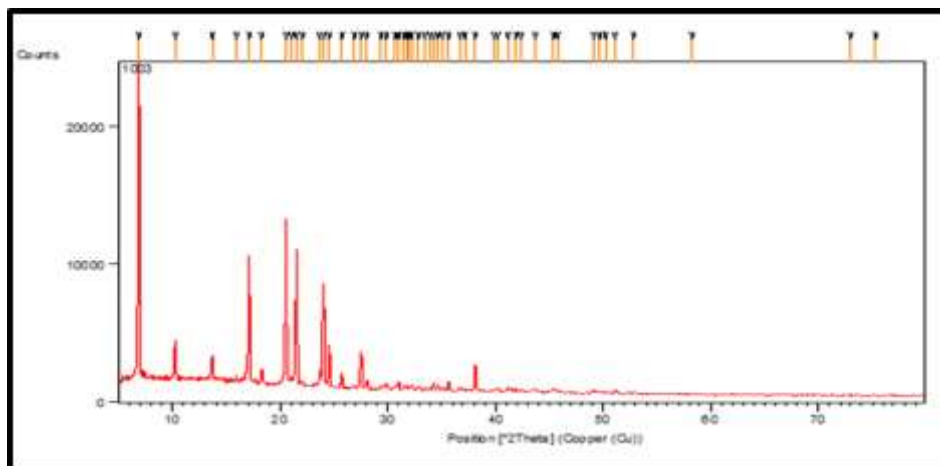

FIGURE 7 XRD diffractogram of sample **SA₁** polymer nanocapsules

Figure 8 displays the XRD diffractogram of sample **SA₂** with its relevant signals. It is notable that the first highest was at 2θ=21.511 with intensity of 100 % and crystal size=33.909 nm. The second highest peak was at 2θ= 21.511 with the intensity of 63.84% and crystal size=32.898. The third highest peak was at 2θ=6.763 with crystal size=46.319. The XRD patterns indicated the increasing number and density of peaks back to the element formation of polymer and amine [19].
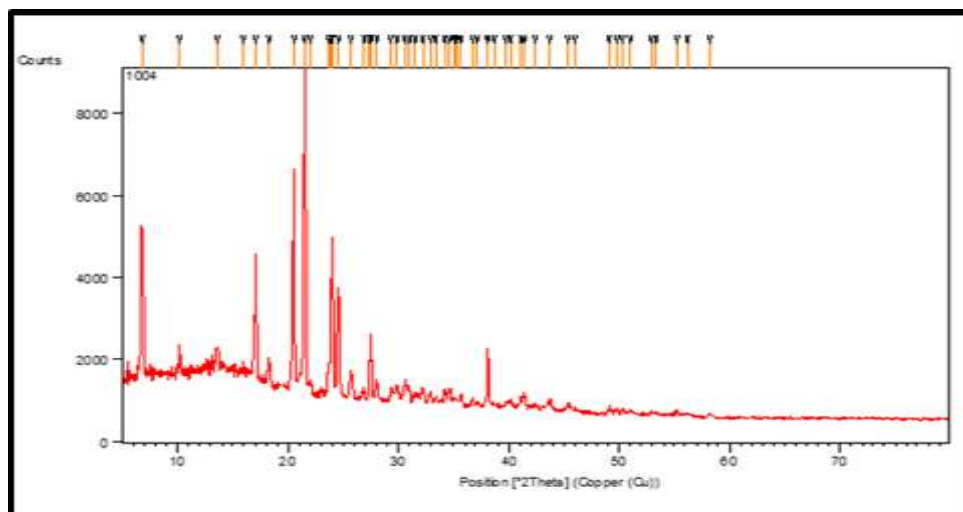

FIGURE 8 XRD diffractogram of sample **SA₂** polymer nanocapsules

Figure 9 indicates the XRD diffractogram of sample **SA₃** with its relevant signals. The first highest peak was observed at 2θ=6.75 with the intensity of 100 % and crystal

size=46.319 nm. The second highest peak was at $2\theta=20.46$ with the intensity of 47.23% and crystal size=49.914. The third highest peak was at $2\theta=17.02$ with the intensity of 46.11%

and crystal size=46.787. Probably the density of peaks returned to the factional groups or molecules from the hybridization, in addition to the peaks of polymer nanocapsule.
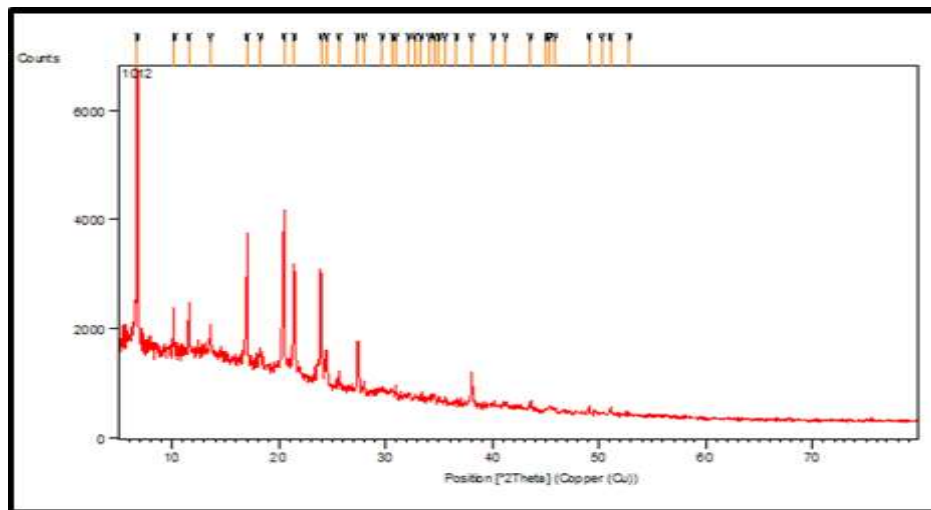

FIGURE 9 XRD diffractogram of sample **SA₃** polymer nanocapsules

Figure 10 demonstrates the XRD diffractogram of sample **SA₄** with broad signals. The first highest peak was appeared at $2\theta=21.91$ with the intensity of 100% and crystal size=80.107 nm. The second highest peak was at $2\theta=6.75$ with the intensity of 59.81% and crystal size=30.285 nm. The

third highest peak was at $2\theta=20.45$ with the intensity of 44.01% and crystal size=49.914 nm. Maybe the density of peaks returned to the factional active groups or molecules from amine, in addition to peaks of polymer nanocapsule [19].
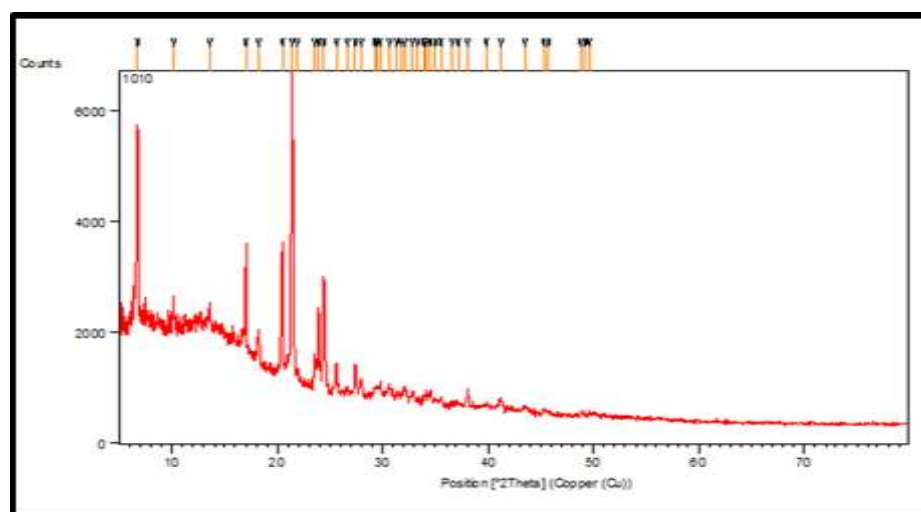

FIGURE 10 XRD diffractogram of sample **SA₄** polymer nanocapsules

Shifting (2θ) and values crystal size for polymer pure and doping are listed in Table 2 in which the best sample doping were

indicated with less crystal sizes as follows: $SA_2 > SA_4 > SA_1 > SA_3$.

TABLE 2 XRD patterns of pure samples polymer and polymer doping with different amine compounds

No.	2Θ	High	d-spacing	FWHM	Intensity %	Crystal Size(nm)
Polymer SA	13.2	592	6.677	2	100	3.956
	30.9	139	2.89	7	23.48	1.165
	42.7	70	2.11	4	11.90	2.110
SA$_1$	6.883	15808	12.832	0.136	100	57.898
	17.104	6850	5.179	0.13	43.33	45.976
	20.55	8649	4.318	0.183	54.72	43.685
	24.010	5515	4.130	0.172	48.47	46.716
	24.53	2500	3.703	0.11	34.89	73.122
SA$_2$	6.763	2501	13.06	0.17	46.42	46.319
	17.082	2065	5.186	0.29	38.34	37.914
	20.54	3439	4.320	0.243	63.84	32.898
	21.311	5387	4.12	0.23	100	33.909
	24.00	2568	3.704	0.2	47.67	40.176
SA$_3$	6.75	3592	8.677	0.17	100	46.319
	17.02	1656	5.20	0.17	46.11	46.787
	20.46	2233	4.33	0.16	62.18	49.914
	21.42	1517	4.14	0.17	42.23	47.073
	23.944	1576	3.71	0.15	43.89	53.568
SA$_4$	6.75	2377	13.079	0.26	59.81	30.285
	17.01	1394	5.208	0.16	35.07	49.661
	20.45	1749	4.338	0.16	44.01	49.914
	21.91	3974	4.053	0.1	100	80.107
	24.42	1522	0.25	0.18	38.30	45.008

Scanning electron microscope of polymer nanocapsules

SEM is considered as one of the most important techniques and is used to examine surface morphology. It has been conducted for polymer acrylic in Figure 11 which has a spherical shape and diameters as (3.164, 4.980, and 11.09) μm.
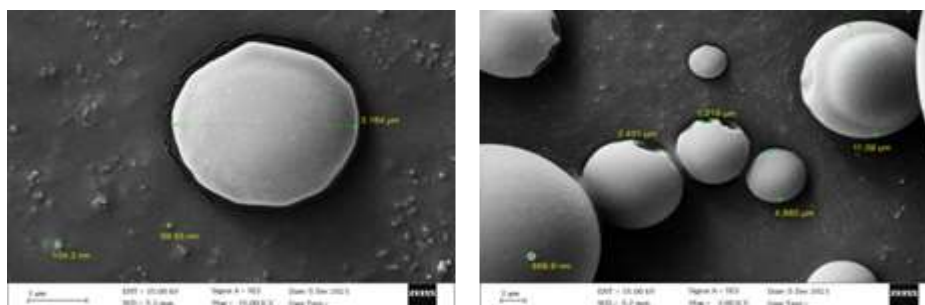

FIGURE 11 SEM image of sample **SA** polymer polyacrylic

The SEM images are depicted in Figure 12 for sample **SA₁**. The morphology presents nanocapsules that are in spherical and irregular shapes, given diameters ranges in nano sizes, in which the images in 100 nm size have diameters values as (67.66, 97.57, 212.5, and 446.3) nm, and the image in 1μm size has the diameter values as about (52.10, 1163.8, 260.5, 469.2, and 511.9) nm.
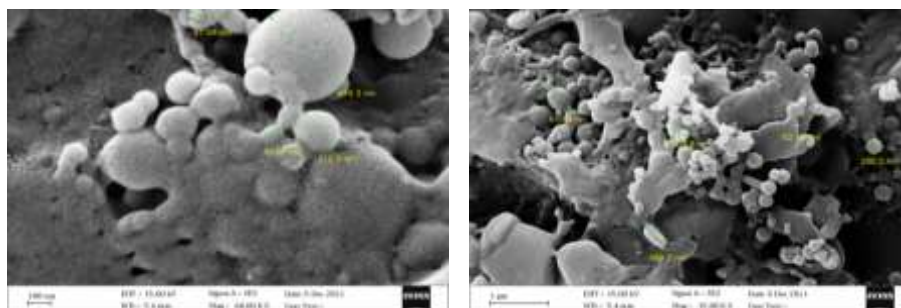
FIGURE 12 SEM Image of sample **SA₁** polymer nanocapsules

The micrograph, in Figure 13, for sample **SA₂** the morphology of nano capsules shows rough white areas as with notable increases at surface. The analysis is performed with dimensions as about (16.75, 72.79, 91.56, 144.8, 165.5, and 197.5) nm in image size of 100 nm, while the diameter values in image 200 nm were as (78.95, 59.55, 89.32, 150.0, and 396.2) nm.
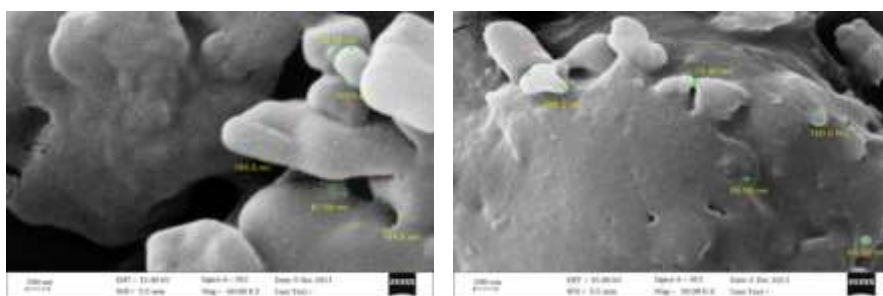

FIGURE 13 SEM Image of sample **SA₂** polymer nanocapsules

The SEM surface morphology of **SA₃** in Figure 14 reveals white areas in spherical shape with diameters as (101.3 and 226.4) nm in image of 100 nm, while, the diameter values in image size of 200 nm were as (68.42, 103.2, and 173.0) nm.
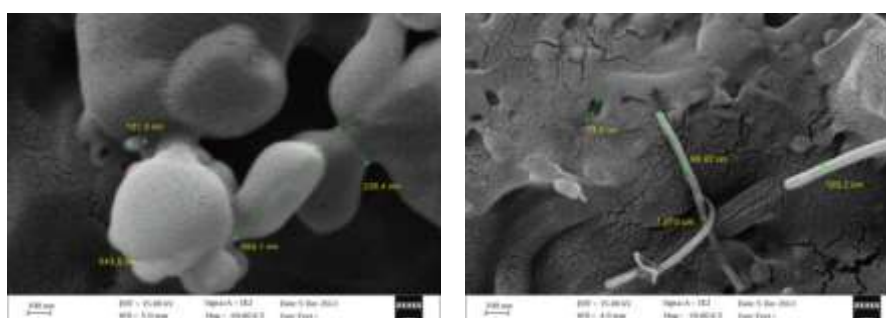

FIGURE 14 SEM Image of sample **SA₃** polymer nanocapsules

The SEM images was demonstrated in Figure 15 for sample **SA₄**. The morphology presents white areas nanocapsules with irregular and spherical shapes having diameters ranges in nano sizes in which the image in 200 nm size have particle sizes as 40.94, 63.27, 139.8, and 402.2 nm, but in image 1μm size, they have 74.43, 209.6, 417.4, 1.632 nm, and 1.839 μm.
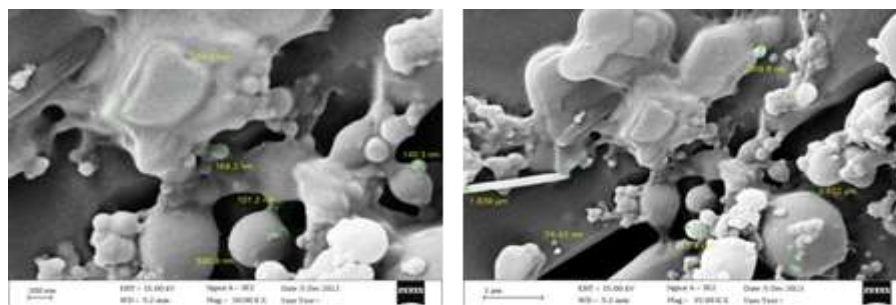
FIGURE 15 SEM Image of sample **SA₄** polymer nanocapsules

Photo-thermal

The results in Figure 16 indicated that temperatures range between 27 and 39 ℃ for nano capsules samples after exposure to IR lamp. However, Figure 17 reveals nano capsules samples returned after exposure to the IR sunlight and temperatures range between 26 and 39 ℃. These figures demonstrated the resulting nano capsules films with a significant photothermal response temperature increasing under sunlight and NIR light irradiation owing to the NIR absorption by the polymers and organic compounds nanomaterials which presented an efficient photothermal temperature range between 27-39 ℃ under NIR irradiation by a commercial IR lamp, but the temperature ranges between 18-26 ℃ was found under IR of sun rays. The nano samples are arranged according to their absorption of sunlight and IR lamp. They are arranged from the highest absorption to the lowest for Nano capsule sample in IR sunlight and IR lamp:**SA₁> SA₂> SA₃>SA₄>SA**. The organic materials with intense absorptions were near IR region (i.e. 750-1300 nm). In this region, a $\pi \rightarrow \pi^*$ transition of electrons was performed containing a double bond methylene C=C that was found in polyacrylic polymer [20]. In addition, propellant chemical groups presented in some samples such as the groups amino $-NH_2$ were found in sample SA_1 and SA_2, but in sample SA_1, the NH_2 orientation compensation at Meta location it acted as a pulling group and led to less absorption in SA_1. Also, the group of hydroxyl-OH was appeared in SA_1, as for the puller group presented in sample SA_2 which contains nitro-NO_2, as well as in SA_3 and SA_4 having strong puller group-NR_3 which leads to the lower absorption to IR ray.

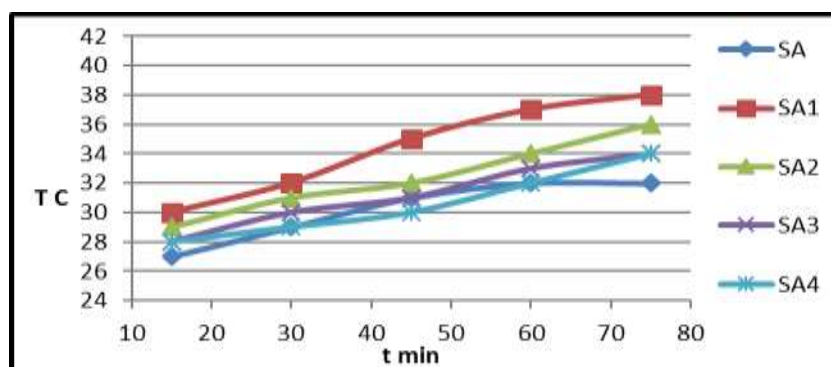**FIGURE 16** Plot of time vs. temperature of samples polymer pure and polymer doped nanocapsule when exposed to IR lamp
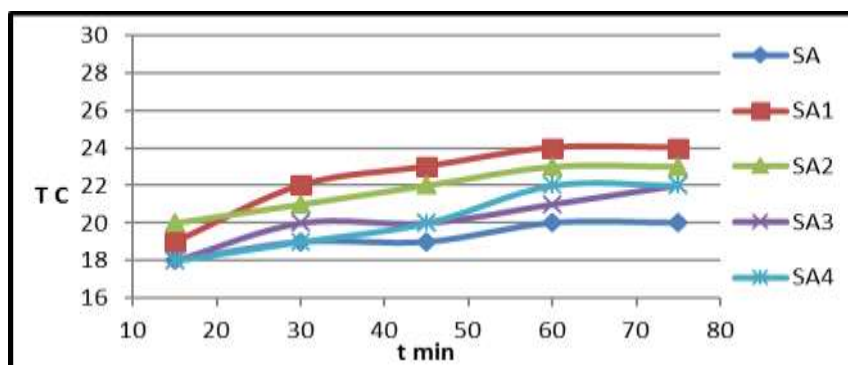
SAMI — Eurasian Chemical Communications

FIGURE 17 Plot of time vs. temperature of samples polymer and doped nanocapsule polymer when exposed to IR sunlight

Conclusion

We deduce the possibility of preparing polyacrylic polymer nanocapsules at nano scale by emulsification method using surfactant CATBr to mix inorganic phase water and organic phase as well as doping the polymers prepared with different amines to improve the absorption photothermal properties of the polymer. The structure of compounds has been identified by Fourier-transform infrared spectroscopy (FT-IR) and proved the existence of new functional group at about 1730 cm^{-1}C=O$_{amide}$ back to reaction between polymer and amines in comparison with FT-IR of pure polymer having C=O$_{carboxylic\ acid}$ at 1622cm^{-1}, in addition to have functional groups of amines and polymer. Using X-ray diffraction (XRD) pattern for the polymer doped led to different scale nanocapsules and it means different doping samples, the crystallite sizes were calculated for samples by using the Scherrer formula that ranged at 17-50 nm. In addition, SEM was utilized to study surface morphology micro particles with high-resolution images of the sample. These images presented surface morphology indicating spherical shapes of white rough areas and agglomeration with irregular shape demonstrating crystals that returned to changes in temperature through preparation. The particles size and diameters were at ranges of 20-200 nm. The films of pure polymer and polymer nanocapsule doped with amines had photothermal properties by ability to absorb IR of sunlight rays and again by IR lamp. That disparity in temperature measurement returned to pulling and propellant groups which directed the samples to absorb rays IR. The nano samples are arranged based on their sunlight absorption and IR lamp. They are arranged from the highest to lowest absorptions of nanocapsule sample in IR sunlight and IR lamp: SA$_1$< SA$_2$< SA$_3$< SA$_4$< SA.

Orcid:

Soraj A. Rahem:
https://www.orcid.org/0000-0002-9287-915X

References

[1] V. Yadav, P. Jadhav, K. Kanase, A. Bodhe, *Int.J. Appl.Pharm.*, **2018**, *10*, 138-146. [crossref], [Google Scholar], [Publisher]
[2] H. Khandelwal, A.P. Schenning, M.G. Debije, *Adv. Energy Mater.*, **2017**, *7*, 1602209. [crossref], [Google Scholar], [Publisher]
[3] S. Patil, A. Choudhary, N. Sekar, P. Pipliya, P. Rathod, *Curr. Trends Fashion Technol. Textile Eng.*, **2019**, *4*, 2577-2929. [crossref], [Google Scholar], [Publisher]

[4] H. Khandelwal, A.P. Schenning, M.G. Debije, *Adv. Energy Mater.*, **2017**, *7*, 1602209. [crossref], [Google Scholar], [Publisher]

[5] C.L. Tan, H. Mohseni, *Nanophotonics*, **2018**, *7*, 169-197. [crossref], [Google Scholar], [Publisher]

[6] K.S. Kumar, V.B. Kumar, P. Paik, *J. Nanoparticles*, **2013**, *2013*, 672059. [crossref], [Google Scholar], [Publisher]

[7] S. Abbas, E. Karangwa, M. Bashari, K. Hayat, X. Hong, H.R. Sharif, X. Zhang, *Ultrason. Sonochem.*, **2015**, *23*, 81–92. [crossref], [Google Scholar], [Publisher]).

[8] P.S. Moreno, Engineering lipid nanocapsule systems for intracellular delivery of anticancer drugs, Ph.D. Dissertation, University of Granada, **2014**. [Pdf], [Google Scholar], [Publisher]

[9] R.N. Mehta, U. More, N. Malek, M Chakraborty, P.A. Parikh, *Appl. Nanosci.*, **2015**, *5*, 891–900. [crossref], [Google Scholar], [Publisher]

[10] K. Subramani, M. Mehta, *Chapter 19- Nanodiagnostics in microbiology and dentistry*, **2018**, 391-419. [crossref], [Google Scholar], [Publisher]

[11] T.F. Chala, C.M. Wu, M.H. Chou, M.B. Gebeyehu, K.B. Cheng, *Nanomaterials*, **2017**, *7*, 191. [crossref], [Google Scholar], [Publisher]

[12] A.C. Veron, Near–Infrared Absorbing Cyanine Dyes and Organic–Inorganic Perovskites for Electronic Applications, Ph.D. Dissertation, University of Zurich Faculty of Science, **2017**. [crossref], [Google Scholar], [Publisher]

[13] B. Koseoglu, methylene blue degradation in water using sol-gel made TiO2 supported oxide Photocatalysts, M.A. Thesis, Engineering and Sciences of University, **2011**. [Google Scholar], [Publisher]

[14] S.B. Said, M.M.A. Mashaly, A.M. Sheta, S.S. Elmorsy, *Int. J. Org. Chem.*, **2019**, *5*, 191-199. [crossref], [Google Scholar], [Publisher]

[15] M.F.H. Al-Kadhemy, Z.S. Rasheed, S.R. Salim, *J. Radiat. Res. Appl. Sci.*, **2016**, *9*, 321-331. [crossref], [Google Scholar], [Publisher]

[16] M. Zhang, S. Zhang, Z. Chen, M. Wang, J. Cao, R. Wang, *Polymers*, **2019**, *11*, 1891. [crossref], [Google Scholar], [Publisher]

[17] M. Todica, T. Stefan, S. Simon, I. Balasz, L. Daraban, *Turk. J. Phys.*, **2014**, *38*, 261-267. [crossref], [Google Scholar], [Publisher]

[18] B. Singh, V. Sharma, *Carbohydr. Polym.*, **2017**, *157*, 185–195. [crossref], [Google Scholar], [Publisher]

[19] R. Balasubramanian, S. Han, C. Chamberlayne, *RSC Adv.*, **2016**, *3*, 11525–11528. [crossref], [Google Scholar], [Publisher]

[20] S. Pascal, S. David, C. Andraud, O. Maury, *Chem. Soc. Rev.*, **2021**, *50*, 6613-6658. [crossref], [Google Scholar], [Publisher]